Mass spectrometric analysis of the kinetics of in vivo rhodopsin phosphorylation

KIMBERLY A. LEE,[1] KIMBERLEY B. CRAVEN,[2] GREGORY A. NIEMI,[1] AND JAMES B. HURLEY[1]

[1]Department of Biochemistry, University of Washington, Seattle, Washington 98195-7350, USA
[2]Department of Physiology and Biophysics, University of Washington, Seattle, Washington 98195-7290, USA

(RECEIVED September 20, 2001; FINAL REVISION December 10, 2001; ACCEPTED December 13, 2001)

Abstract

On stimulation, rhodopsin, the light-sensing protein in the rod cells of the retina, is phosphorylated at several sites on its C terminus as the first step in deactivation. We have developed a mass spectrometry–based method to quantify the kinetics of phosphorylation at each site in vivo. After exposing either a freshly dissected mouse retina or the eye of an anesthetized mouse to a flash of light, phosphorylation and dephosphorylation reactions are terminated by rapidly homogenizing the retina or enucleated eye in 8 M urea. The C-terminal peptide containing all known phosphorylation sites is cleaved from rhodopsin, partially purified by ultracentrifugation, and analyzed by liquid chromatography coupled with mass spectrometry (LCMS). The mass spectrometer responds linearly to the peptide from 10 fmole to 100 pmole. The relative sensitivity to peptides with zero to five phosphates was determined using purified phosphopeptide standards. High pressure liquid chromatography (HPLC) coupled with tandem mass spectrometry (LCMS/MS) was used to distinguish the three primary sites of phosphorylation, Ser 334, Ser 338, and Ser 343. Peptides monophosphorylated on Ser 334 were separable from those monophosphorylated on Ser 338 and Ser 343 by reversed-phase HPLC. Although peptides monophosphorylated at Ser 338 and Ser 343 normally coelute, the relative amounts of each species in the single peak could be determined by monitoring the ratio of specific daughter ions characteristic of each peptide. Doubly phosphorylated rhodopsin peptides with different sites of phosphorylation also were distinguished by LCMS/MS. The sensitivity of these methods was evaluated by using them to measure rhodopsin phosphorylation stimulated either by light flashes or by continuous illumination over a range of intensities.

Keywords: Phosphorylation; mass spectrometry; rhodopsin; G protein–coupled receptor; kinetics

Protein phosphorylation plays a key role in a wide variety of cellular functions (Koch et al. 1991; Graves and Krebs 1999). The universal role of phosphorylation is illustrated by the hundreds of protein kinases and phosphatases that have been found in the genomes of eukaryotic organisms (Hunter and Plowman 1997; Plowman et al. 1999; Adams et al. 2000). The rapidly reversible nature of this post-translational protein modification allows for dynamic signaling in a variety of systems, but its transient nature makes the detailed study of phosphorylation a complex problem.

The most common method for study of phosphorylation traditionally has involved the use of radiolabeling, both in vitro and in vivo. This method has proven very sensitive and effective in well-controlled in vitro studies, but in vivo experiments are considerably more difficult to control. Radiolabel uptake may be variable, and the presence of prebound unlabeled phosphate cannot be quantified. Another common

Reprint requests to: James B. Hurley, Box 357350, University of Washington, Seattle, WA 98195; e-mail: jbhhh@u.washington.edu; fax: (206) 685-2320.

Abbreviations: LCMS, liquid chromatography mass spectrometry; CID, collision-induced dissociation; MS/MS, tandem mass spectrometry utilizing CID; Asp-N, endoproteinase Asp-N; HEPES, N-[2-hydroxyethyl]piperazine-N′-[2-ethanesulfonic acid]; EDTA, ethylenediamine-tetraacetic acid; ROS, rod outer segments; ID, internal diameter; HFBA, heptafluorobutyric acid; GPCR, G protein–coupled receptor; PS334, pS338, pS343, pT340, rhodopsin C-terminal peptides phosphorylated on Ser 334, Ser 338, Ser 343, and Thr 340, respectively.

Article and publication are at http://www.proteinscience.org/cgi/doi/10.1110/ps.3870102.

technique, the use of specific phosphoamino acid antibodies is very useful in initial studies, but because unphosphorylated species are not detected, stoichiometric measurements cannot be made.

Mass spectrometry has become an effective alternative method to analyze protein phosphorylation (Annan and Carr 1996; Carr et al. 1996; Resing and Ahn 1997; Neubauer and Mann 1999; Oda et al. 1999). The use of mass spectrometry allows for fast analysis of many phosphorylated peptides in complex mixtures. Samples derived from in vivo experiments also can be analyzed by mass spectrometry, without the difficulties and uncertainties associated with metabolic labeling. Several recent reports have focused on methodology for cataloging the phosphoproteome, the components of the proteome that become phosphorylated (Goshe et al. 2001; Oda et al. 2001; Vener et al. 2001; Zhou et al. 2001). Identification of phosphorylated proteins and their sites of phosphorylation is a first step in understanding the numerous biological roles of protein phosphorylation. However, once potential sites of phosphorylation of a protein are identified, the function of the modification still needs to be defined. Determination of the stoichiometry of phosphorylation under different cellular conditions and the kinetics of phosphorylation and dephosphorylation in response to a stimulus provide essential information about the function of the phosphorylated protein.

In this study, we rigorously examine the phosphorylation of rhodopsin, a G protein–coupled receptor (GPCR) known to be phosphorylated at its C terminus in response to a stimulus. The C-terminal peptide of mouse rhodopsin that we analyzed contains six sites of phosphorylation, adding to the complexity of analysis.

Photoactivation of rhodopsin is the trigger for phototransduction, the signaling cascade in a rod photoreceptor cell. A key step in the inactivation of phototransduction in rods is rhodopsin phosphorylation (for review, see Hurley et al. 1998). We recently used mass spectrometry to show that the kinetics and extent of phosphorylation of rhodopsin in vivo are important for deactivation of phototransduction and dark adaptation (Kennedy et al. 2001). Rhodopsin is an integral membrane protein, but its C terminus can be solubilized by cleaving it from the protein with endoproteinase Asp-N (Asp-N). This produces a soluble 19-amino-acid peptide containing all known phosphorylation sites (Palczewski et al. 1991). We developed a mass spectrometry method to quantify peptides with zero, one, two, three, four, and five phosphates. Using high pressure liquid chromatography (HPLC) separation and comparisons of characteristic ms/ms daughter ion intensities, we also determined the relative quantities of species of the same molecular mass but different phosphorylated sites.

In this report, we describe in detail how this method can be applied to samples produced from mouse retinas using two variations of a novel rapid-quench protocol. Mouse retinas were used because mice can be readily dark-adapted, because their retinas are highly enriched with rod photoreceptors, and because numerous transgenic lines of mice are available. In the first method, a light flash is administered to a dissected retina to initiate rhodopsin phosphorylation. The reaction is quickly terminated by homogenization in urea. The second protocol is performed completely in vivo, with light continuously illuminating the eye of an anesthetized mouse, followed by euthanasia then rapid enucleation and homogenization of the whole eyeball in urea to terminate phosphorylation and dephosphorylation reactions. Endoproteinase Asp-N was used to cleave the C terminus of rhodopsin, generating a peptide containing all known phosphorylation sites (Palczewski et al. 1991). A range of light intensities was used for each study, and the threshold for detection of rhodopsin phosphorylation was determined.

The methodology outlined in this report can be adapted and applied to numerous biological systems for the rigorous analysis of in vivo phosphorylation in very complex or more standard phosphorylation patterns.

Results

Linearity of response

We used synthetic rhodopsin C-terminal peptides to show that the response of the mass spectrometer is linear with respect to quantity of peptide injected within the range of concentration used in our experiments. Doubly charged peptides were monitored, as singly and triply charged rhodopsin peptide ions were not observed under our conditions. The liquid chromatography coupled with mass spectrometry (LCMS) response was linear in the range from 10 fmole to 100 pmole of monophosphorylated (pS338) peptide and from 1 to 100 pmole for unphosphorylated peptide by LCMS (Fig. 1). For the data points shown in Figure 1A, 1–100 pmole in *N*-[2-hydroxyethyl]piperazine-*N*′-[2-ethanesulfonic acid] (HEPES) buffer were injected directly onto the column. To acquire the data shown in Figure 1B, with 10 fmole to 1 pmole monophosphorylated peptide, the indicated quantity of peptide was added to 5 μL of Asp-N digested mouse retinal sample (~30 pmole rhodopsin), which served as background and carrier protein, simulating a real sample from our analyses. These samples were prepared as described within the Materials and Methods section, with no light administered. The linearity of the mass spectrometric signal for peptides injected both in HEPES buffer and in the retinal sample indicates that the presence of other peptides in the sample does not affect the linearity of the signal.

All conditions of analysis, including all HPLC conditions, all instrument voltages, and the exact microspray needle position, were held constant for each set of data points. The raw number of counts for each peptide was

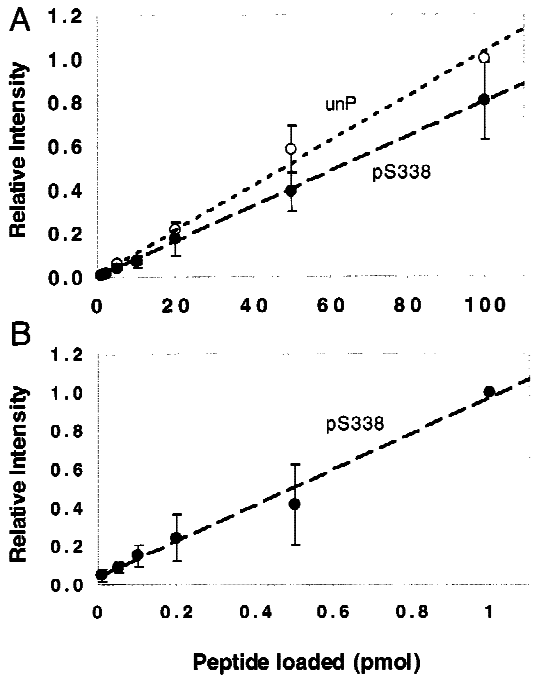

Fig. 1. Linearity of mass spectrometric signal with respect to quantity of peptide injected for unphosphorylated and monophosphorylated mouse rhodopsin peptide analyzed by LCMS. (*A*) One to 100 pmole synthetic unphosphorylated (unP, open circles) and monophosphorylated (pS338, filled circles) peptide. The signal for the indicated amount of each peptide was divided by the signal produced by 100 pmole of the unphosphorylated peptide to generate the relative signal that is plotted. The relative value of 1 corresponds to 2.0×10^{10} mass spectrometric counts. All peptides were in 10 mM HEPES at pH 7.4. (*B*) Ten femtomoles to 1 pmole monophosphorylated peptide (pS338). The signal for indicated amount of each peptide was divided by the signal produced by 1 pmole of the peptide to generate the relative signal shown. The relative value of 1 corresponds to 1.5×10^9 counts. The peptide was spiked into mouse retinal sample for analysis. For all data sets, the best linear fit is plotted, and error bars represent standard deviations of three experiments.

recorded and plotted. Because the response was linear over the full range of values, we conclude that the instrument has not reached its saturation level. This demonstration of linearity of mass spectrometric signal with peptide concentration validated our strategy of correlating response levels with peptide concentration in our analyses of rhodopsin phosphorylation.

Effect of pH on peptide detection

Phosphorylated peptides are not detected as efficiently by mass spectrometry as their unphosphorylated counterparts. Phosphate groups may not be protonated well, even under the highly acidic conditions used for mass spectrometric analysis. Because the mass spectrometer was used in positive ion mode for all analyses, any peptides with phosphate groups that were not fully protonated would not be detectable. This hypothesis predicts that the efficiency of detection of a phosphopeptide relative to its unphosphorylated counterpart will vary directly with the concentration of protons in the solution. To test the hypothesis, we measured the mass spectrometric signal for a 10-pmole/μL solution of the rhodopsin C-terminal peptide unphosphorylated and with five phosphates at three different acidic pH levels. Previous work had focused on the relative sensitivity of the instrument to monophosphorylated peptides at either low pH or the very high pH used for negative ion mode (Carr et al. 1996; Wilm et al. 1996; Neubauer and Mann 1999). As predicted, the lowest pH solution yielded the highest sensitivity to the phosphopeptide relative to the unphosphorylated peptide, whereas the mixture with the highest pH had the lowest relative efficiency of detection of the doubly charged phosphopeptide (Fig. 2A).

The sensitivity of the instrument to the unphosphorylated peptide at the three pH conditions also was measured. The instrument consistently detected the unphosphorylated peptide with the highest efficiency at the highest pH, whereas the efficiency of detection decreased at lower pH (Fig. 2B). Because this is opposite of the effect of pH on the phosphorylated peptides, the decrease in relative sensitivity to the phosphopeptide is not simply caused by a decrease in total sensitivity of the mass spectrometer at high pH.

Relative responses of different phosphorylated forms of the rhodopsin C-terminal peptide

The relative responses of the mass spectrometer to synthetic rhodopsin peptides with zero to five phosphates were determined by LCMS (Fig. 2C). Sensitivity coefficients were calculated for each phosphorylation state, and these values were used to convert relative observed responses of the mass spectrometer to relative quantities for each phosphorylated species present in the sample.

To determine these coefficients, we first measured the effects of phosphorylation on detection of peptides cleaved from the bovine rhodopsin C terminus. Bovine peptides were used because mouse synthetic peptides were unavailable, and bovine retinas are readily available in large quantities. Bovine peptides with zero to five phosphates were generated from rod outer segment preparations (ROSs). These peptides were purified by HPLC and quantified by amino acid analysis (AAA Laboratories), and their purity was assessed by HPLC and mass spectrometry. Equal quantities of peptides of each phosphorylation state (zero to five phosphates) were combined and analyzed by LCMS. After adjustment for purity, the mass spectrometric signal for the peptide of each phosphorylation state was divided by the unphosphorylated peptide signal to calculate the relative sensitivity of the instrument to the bovine phosphopeptide with one to five phosphates (open circles in Fig. 2D).

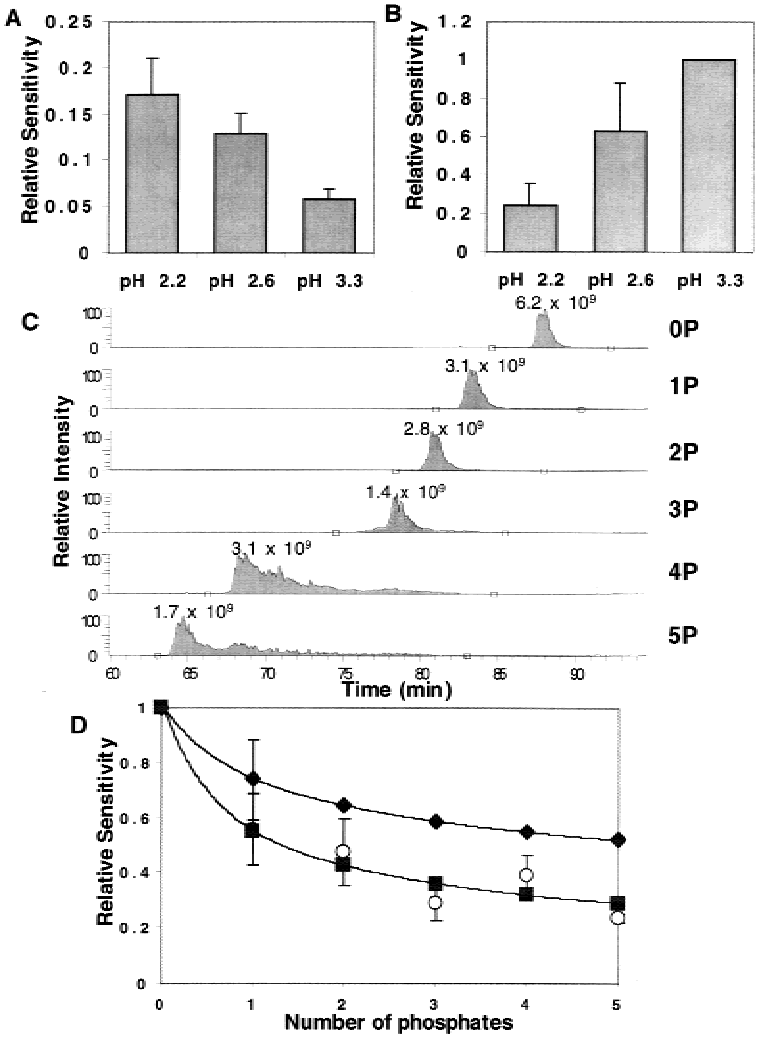

Fig. 2. Relative sensitivity of the mass spectrometer to various phosphorylation states of rhodopsin C-terminal peptide. (*A*) Change in relative sensitivity of the mass spectrometer to a doubly charged phosphopeptide at various pH levels. Solutions containing bovine unphosphorylated rhodopsin C-terminal peptide and the same peptide with five phosphates, each at 10 pmole/μL, at three different pH levels, was infused directly into the mass spectrometer at 1 μL/min. The signal from each peptide was integrated, and the phosphopeptide signal was divided by the signal from the unphosphorylated peptide to calculate the relative efficiency. Error bars represent standard deviation. Each replicate represents a solution individually made and analyzed. pH 2.2, n = 3; pH 2.6, n = 4; pH 3.3, n = 4. (*B*) Change in efficiency of detection of doubly charged unphosphorylated peptide at different pH levels. Using the same data, we compared the mass spectrometric signal for the unphosphorylated rhodopsin C-terminal peptide at each of the three pH levels. For each set of solutions analyzed on the same day, the relative efficiency of detection of the unphosphorylated peptide was determined, with the highest signal being assigned a value of one. The average of four data sets (three for pH 2.2) is plotted, with error bars representing standard deviation. (*C*) Ion chromatograms of bovine rhodopsin C-terminal peptides. Five picomoles of each phosphorylation state of bovine rhodopsin (zero to five phosphates) was analyzed by LCMS. The x-axis represents elution time, and the y-axes are intensity of signal. The chromatograms pictured represent the same LCMS run, with the data divided into different mass windows. Each panel represents a different phosphorylated form of the peptide, from zero (0P) to five (5P) phosphates. The doubly charged ion of each phosphorylated species was monitored. Mass windows used are 2.5 Daltons wide, monitoring m/z = 969.7 for unphosphorylated, with the m/z increasing 40 units for each additional phosphate. The peak areas were integrated, with the area displayed above the peak. (*D*) Determination of sensitivity coefficients for mouse peptides. The relative sensitivity of the mass spectrometer to each bovine phosphorylated species was determined by dividing the signal observed for that species by the signal for the unphosphorylated peptide (open circles, error bars represent the standard deviation of six replicates). The curve fit to these data is shown (filled squares). The same equation was used to fit the mouse monophosphorylated peptide sensitivity data and predict the sensitivity coefficients for mouse peptides with two to five phosphates (filled diamonds). Error bars for mouse monophosphorylated sensitivity represent standard deviation of 29 replicates.

A similar analysis then was performed on the synthetic mouse rhodopsin C-terminal peptide phosphorylated on Ser 338. Although only pS338 was used in this analysis, all three synthetic monophosphorylated mouse peptides were detected with the same efficiency (data not shown). The sensitivity of the mass spectrometer to the monophosphorylated peptide was determined by injecting equal quantities (10 fmole to 100 pmole) of unphosphorylated and pS338 synthetic mouse peptide, running LCMS using our standard chromatography conditions, and observing the peak areas for the phosphorylated and unphosphorylated peptide masses. These data from the mouse peptide were used to correct the model generated from the bovine data (Fig. 2D).

First, an equation was generated to fit the bovine data:

$$E_P = E_{P-1}\left(1 - \frac{F_b}{P}\right) \quad (1)$$

E_P represents the efficiency of detection of a peptide with P phosphates, and F_b represents the sensitivity reduction factor for the bovine peptide. This equation is based on the hypothesis that the reduction in efficiency is proportional to the fractional increase in negative charge brought about by addition of a phosphate. Figure 2D shows that this equation provided a reasonable fit to the data. F_b was determined to be 0.45 by best fit of the bovine data.

This equation then was used to calculate the predicted efficiencies of detection for multiply phosphorylated mouse peptides. The sensitivity reduction factor for the mouse peptide (F_m) was calculated by using the experimentally determined value for the efficiency of detection of the monophosphorylated mouse peptide ($E_1 = 0.74$) and solving the equation for F_m. With the efficiency of detection of unphosphorylated peptide (E_0) defined as 1, F_m was determined to be 0.26. This value was used in equation 1 to calculate the

multiply phosphorylated peptide efficiencies of detection. The calculated sensitivity coefficients are 0.74, 0.64, 0.59, 0.55, and 0.52 for one through five phosphate-containing peptides, respectively. This equation may be applicable to any peptide, requiring only the determination of the sensitivity reduction factor F for that peptide.

Phosphorylation site determination

Sites of phosphorylation of both the singly and doubly phosphorylated species in mouse retinal samples were determined by HPLC coupled with tandem mass spectroscopy. Initially, MS/MS was performed with synthetic monophosphorylated peptides directly infused into the mass spectrometer so that the best instrument settings for LCMS analysis could be determined. Fragmentation conditions, including activation energy, activation time, and the mass window of activation, were all optimized to provide the most useful daughter ion spectrum. Values for the instrument's fragmentation settings are listed in the Materials and Methods section.

MS/MS spectra from each of the monophosphorylated synthetic mouse rhodopsin C-terminal peptides (pS334, pS338, and pS343) are shown in Figure 3, along with predicted masses of the b series of daughter ions from each peptide. Because rhodopsin peptides monophosphorylated at different sites all have the same mass, we used tandem mass spectrometry to identify the sites of phosphorylation.

Some daughter ions are formed from all these monophosphorylated isoforms. These are the fragments of low or high mass, which contain either none or all of the possible phosphorylation sites. These daughter ions are useful in identifying the peptide as monophosphorylated rhodopsin C terminus, but they give no information about the site of phosphorylation.

Daughter ions resulting from fragmentation events between potential phosphorylation sites are more useful for determining the site of phosphorylation of the peptide. Certain daughter ions, boldface in Figure 3, are unique to particular phosphorylation sites on the parent peptide. For example, a daughter ion of m/z = 1293.5 is prominent as the b_{13} ion in the ms/ms spectrum of pS343. The b_{13} ion from

A

b ions 1 2 3 4 5 6 7 8 9 10 11 12 13 14 15 16 17 18 19

NH_3^+ · D · D · D · A · S · A · T · A · S · K · T · E · T · S · Q · V · A · P · A · COOH

	pS334	pS338	pS343
b_1	116.035	116.035	116.035
b_2	231.062	231.062	231.062
b_3	346.089	346.089	346.089
b_4	417.126	417.126	417.126
b_5	**584.124**	*504.158*	*504.158*
b_6	**655.161**	*575.195*	*575.195*
b_7	**756.209**	*676.243*	*676.243*
b_8	**827.246**	*747.28*	*747.28*
b_9	*914.278*	*914.278*	**834.312**
b_{10}	*1042.373*	*1042.373*	**962.407**
b_{11}	*1143.421*	*1143.421*	**1063.454**
b_{12}	*1272.463*	*1272.463*	**1192.497**
b_{13}	*1373.511*	*1373.511*	**1293.545**
b_{14}	1460.543	1460.543	1460.543
b_{15}	1588.602	1588.602	1588.602
b_{16}	1687.67	1687.67	1687.67
b_{17}	1758.707	1758.707	1758.707
b_{18}	1855.76	1855.76	1855.76
b_{19}	1926.797	1926.797	1926.797

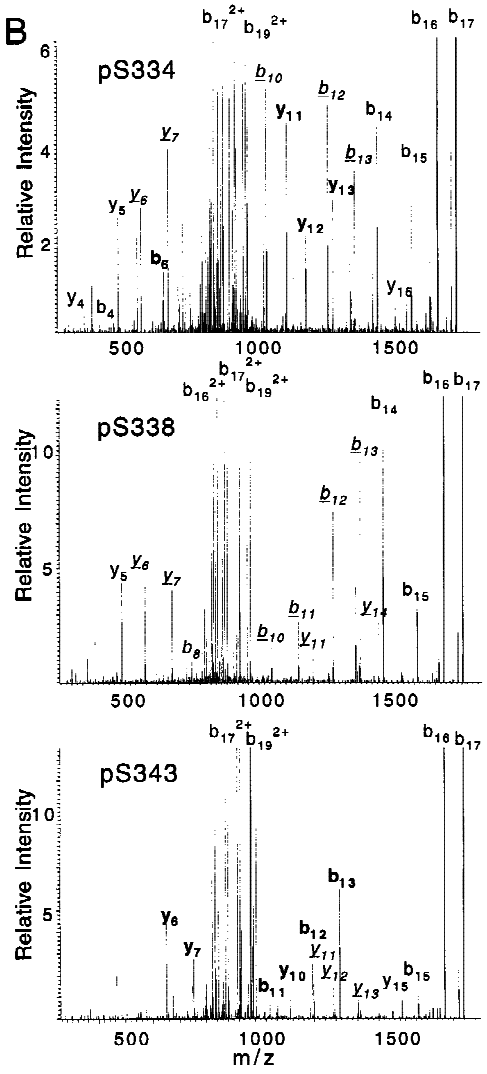

Fig. 3. Phosphorylation site determination of monophosphorylated rhodopsin peptides. (*A*) Amino acid sequence of mouse rhodopsin C-terminal peptide resulting from Asp-N cleavage and the predicted b ions resulting from fragmentation of each of the three serine-monophosphorylated peptides. (*B*) Tandem mass spectra from synthetic rhodopsin peptides monophosphorylated on the three serine residues. Spectra were collected by direct infusion of the synthetic peptide solution into the mass spectrometer. Each spectrum is an average of 30 scans. Parent ions are doubly charged. In both *A* and *B*, daughter ions unique to one site of phosphorylation are indicated in boldface, and daughter ions indicative of a subset of potential phosphorylation sites, but not unique to one site, are italicized and underlined.

rhodopsin monophosphorylated on any site other than Ser 343 has a mass of 1373.5 because it includes the phosphate.

Only pS334 and pS343, the peptides monophosphorylated on either the first or last possible phosphorylation site, produce unique daughter ions. pS338 and all peptides monophosphorylated on threonine residues must be identified by studying the combination of indicative daughter ions (underlined in Figure 3) that are present in the spectrum, as well as noting those that are absent.

Using the synthetic monophosphorylated mouse rhodopsin peptide standards, we developed an LCMS-based method for quantifying the relative amount of each monophosphorylated species in actual retinal samples. We found that under normal HPLC conditions pS334 eluted separately from pS338 and pS343 (Fig. 4A). Therefore, we were able to determine the relative amount of pS334 by integrating this separate peak and comparing its area with the area of the unphosphorylated peptide peak. Under our best chromatography conditions, the pS338 and pS343 peptide peaks were partially separated (Fig. 4B).

Additionally, low levels of peptides monophosphorylated on Thr 340 were observed. The small amount of pT340 peptide provided a ms/ms spectrum of sufficient quality to narrow the site of phosphorylation to either Ser 338 or Thr 340 (Fig. 4C). Specifically, the strong y_{11} ion of m/z = 1198 placed the site of phosphorylation on Ser 338, Thr 340, Thr 342, or Ser 343, whereas the prominent b_{12} ion containing the phosphate (m/z = 1272) indicated that the site of phosphorylation was not Thr 342 or Ser 343. These conclusions were supported by several other ions in the spectrum. However, the ions that would discriminate between pS338 and pT340 and firmly identify the parent peptide's phosphorylation site (b_9, b_{10}, y_9, and y_{10}) were not present in the spectrum in sufficient abundance to make a conclusive determination.

However, the second distinct monophosphorylated peak to elute contained sufficient peptide to definitively identify its site of phosphorylation as solely Ser 338. The ions listed above that identify the parent peptide as either pS338 or pT340 were observed, but the b_9, b_{10}, y_9, and y_{10} fragments were also present in the spectrum. All of these ions identified the phosphorylation site as Ser 338, indicating that the first peak to elute must contain only pT340.

Although optimal peptide separation would be desirable at all times, it usually requires sample run times in excess of 2 h and constant adjustment of HPLC gradient and flow rate. Thus, optimal peptide separation proved impractical for the type of high-throughput analysis required by the nature of our experiments.

The pS338 and pS343 peptides coelute under our standard chromatography conditions. To determine the relative quantities of these peptides, we monitored the ratio of the b_{13} ions characteristic of each phosphorylated species. The b_{13} ion of m/z = 1293 is unique to the pS343 phosphorylated species and therefore is positively indicative. The b_{13} ion produced from pS338 is common to pS338, pS334, and all rhodopsin C-terminal peptides monophosphorylated on threonine residues. However, because pS334 elutes as a separate peak, and because we have only observed trace levels of threonine-phosphorylated rhodopsin peptides, we feel confident in assigning any detected daughter ion of m/z = 1376 in this peak to the pS338 parent ion. Because the b_{13} ions from the various peptides are produced with different efficiencies, it is necessary to incorporate a correction factor. To determine the value of this factor (x), we analyzed standard mixtures containing both pS338 and pS343 at varying ratios. The calculated fractions of each peptide were determined using the following equations, where A represents the integrated area of each daughter ion peak:

$$\text{Calculated \% pS338} = \frac{A_{\text{pS338b13}}}{xA_{\text{pS343b13}} + A_{\text{pS338b13}}} \quad (2)$$

$$\text{Calculated \% pS343} = \frac{xA_{\text{pS343b13}}}{xA_{\text{pS343b13}} + A_{\text{pS338b13}}} \quad (3)$$

The calculated fraction of each peptide was plotted against the actual fraction of that peptide in the standard mixture (Fig. 4D). The best fit value for x was determined by linear regression to be 2.1.

We also determined the primary phosphorylation sites of doubly phosphorylated rhodopsin peptides (Fig. 5). Using our standard liquid chromatography conditions, we were unable to separate doubly phosphorylated rhodopsin C-terminal peptides into distinct species. It therefore was necessary to use LCMS/MS to determine the primary phosphorylation sites of the heterogeneous doubly phosphorylated peak.

To optimize fragmentation conditions for doubly phosphorylated peptides, several values for the activation amplitude initially were used to fragment the doubly phosphorylated peptide peak in each sample, and the resulting series of ms/ms spectra were compared. The activation amplitude that gave the most useful daughter ion spectra was determined to be 28.0%, and this value was used through the course of the study. Other fragmentation settings of the ion trap were the same as those used for ms/ms of monophosphorylated peptides.

Masses of b and y ions predicted for all possible doubly phosphorylated rhodopsin parent ions were monitored. The relative intensities of each of these daughter ions were used to determine the primary phosphorylation sites of doubly phosphorylated rhodopsin in each sample. In samples from highly bleached mouse retinas, we found that very soon after light exposure the primary sites of double phosphorylation are Ser 343 and Ser 338, but later peptides phosphory-

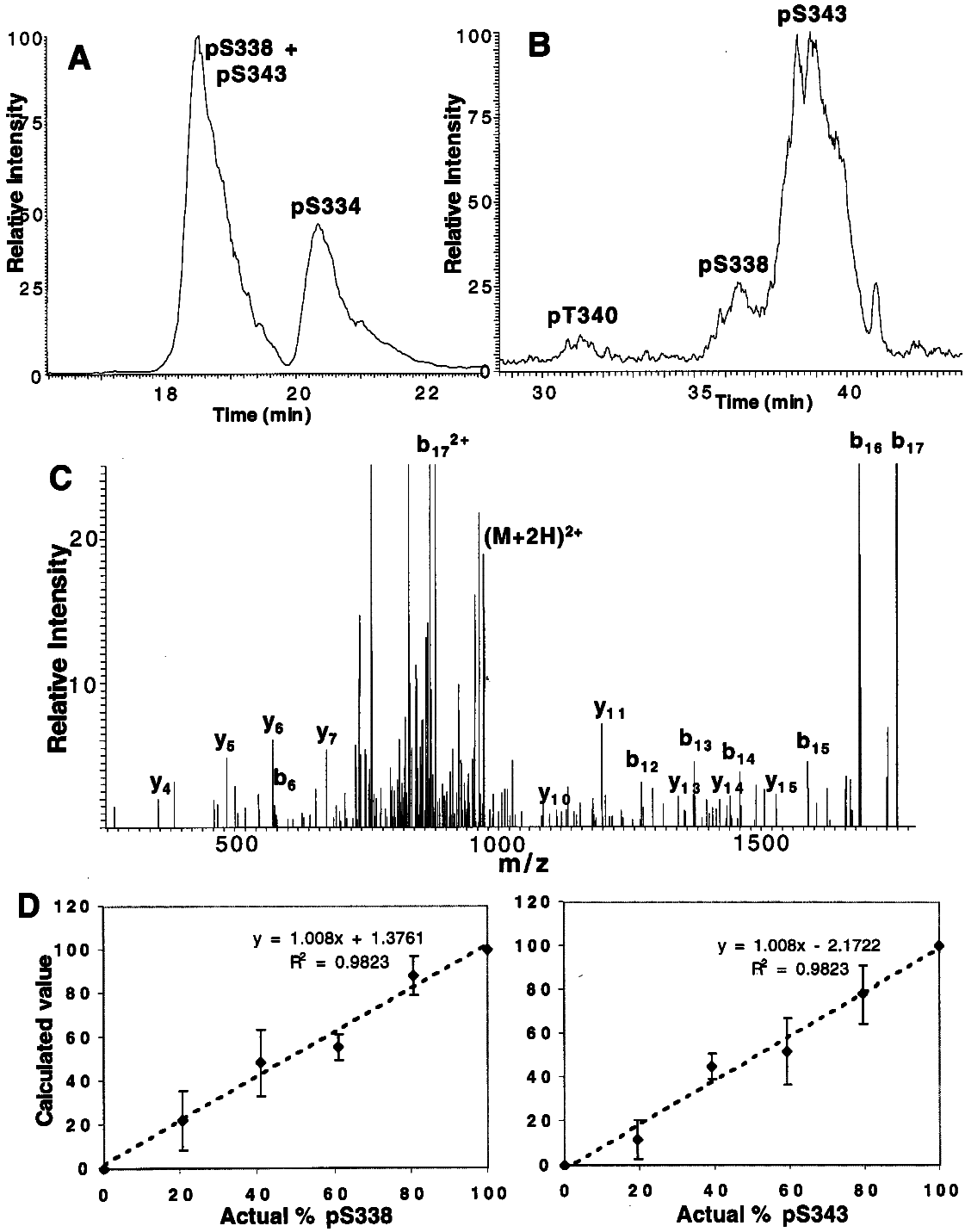

Fig. 4. Relative quantitation of various monophosphorylated peptides. (*A*) Ion chromatogram of pS334, pS338, and pS343 under standard chromatographic conditions. Equal quantities of each synthetic monophosphorylated peptide were analyzed, and total ion current is pictured. (*B*) Ion chromatogram of the monophosphorylated components of mouse retinal sample under optimal chromatographic conditions. The three peaks corresponding to different monophosphorylated species are labeled. pS334 was not present in this early time point sample in significant quantity. Doubly charged ions were monitored (m/z = 973.3). (*C*) MS/MS spectrum of the pT340 peak in *B*. b and y ions are labeled, and $(M + 2H)^{2+}$ represents the doubly charged parent ion (m/z = 973.3). (*D*) Determining the fraction of pS338 or pS343 peptide by measuring the b_{13} ion signal. Mixtures of the two peptides at known proportions were analyzed by LCMS/MS. The fraction of peptide in each phosphorylation state was calculated using equations 2 and 3. The calculated percentage of each peptide is plotted against the known fraction of that peptide in the sample mixture. The equations for the best-fit lines and the R^2 values (square of the Pearson product moment correlation coefficient) are indicated. Error bars represent standard deviations from three experiments.

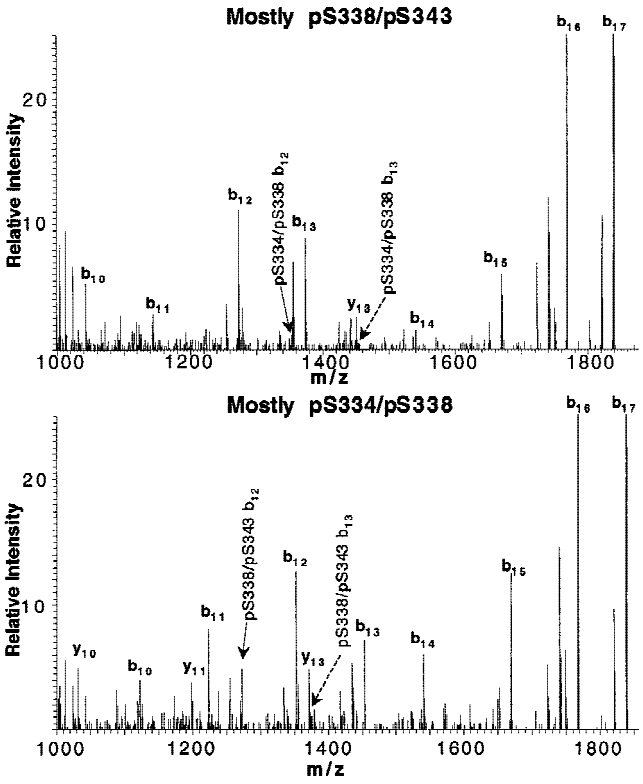

Fig. 5. Determination of phosphorylation sites of doubly phosphorylated peptides by tandem mass spectrometry. Spectra from the higher mass range (1000–1850 m/z) of mouse retinal samples with various primary sites of phosphorylation are presented. The b and y ions produced by the indicated doubly phosphorylated peptide (pS338/pS343 in the top panel, pS334/pS338 in the bottom panel) are labeled in both panels. For comparison, the positions of the b_{12} and b_{13} ions predicted for peptides doubly phosphorylated on other potential sites also are indicated on each spectrum. Parent ions are doubly charged (m/z = 1013.3) Each spectrum is an average of ~350 scans over 3.5 min.

lated on Ser 334 and Ser 338 were also present (Kennedy et al. 2001).

Use of internal standards

We used bovine rhodopsin phosphopeptides as internal standards in an attempt to reduce the variability of the data from each of the sample preparation protocols. An equal amount of light-exposed bovine ROS (see Materials and Methods for details of preparation) was added to each sample after it was thawed but before the first centrifugation and washing step in the sample preparation. The ROSs then were washed along with the mouse retina or eye sample, the C-terminal peptide of the bovine rhodopsin was cleaved in the same reaction as the mouse peptide, and the amount of bovine peptide of each phosphorylation state in each sample was determined by LCMS as the mouse samples were analyzed (Fig. 6). Adding the ROS standard at this point in the protocol allowed us to correct for any loss during the washing steps, differences in protease cleaving efficiency, and any differences in analytical efficiency during LCMS. As will be described in a later section, use of the internal standard did not improve the reproducibility of the results.

Sensitivity of this method using phosphorylated rhodopsin peptides purified from mouse retina

To test the sensitivity of our method, retinal peptide samples were prepared by the rapid-quench protocol described above, using light flashes of 0.009–0.9 mJ/cm^2. Reactions were terminated 2 sec after the flash. We observed that the dimmest flash, 0.009 mJ/cm^2, elicited a phosphorylation response that was similar to the amount of phosphorylation present when no flash is administered. However, the flashes of 0.09 and 0.9 mJ/cm^2 resulted in significantly increased levels of both monophosphorylated and diphosphorylated rhodopsin peptides (Fig. 7). Note that although the level of phosphorylated peptide is much lower than that of unphosphorylated rhodopsin peptide, the phosphorylated species are easily detectable by our method.

We also studied the phosphorylation that results from prolonged exposure to a light stimulus using the in vivo protocol described above. After 2 min of continuous light stimulation, we also observed phosphorylation levels similar to those observed without light stimulus when administering dim illumination (0.001 mW/cm^2 or less, Fig. 8). Between 0.001 and 0.01 mW/cm^2 a significant increase in phosphorylation levels was observed, with relative amounts of mono-, di-, and triphosphorylated peptides increasing. This trend continued with increasing light intensities. Under these conditions, using 1.0 mW/cm^2 illumination, we commonly observed up to five phosphates on a single rhodopsin C-terminal peptide (Fig. 8).

Discussion

Previous studies performed in vitro have shown that rhodopsin can be multiply phosphorylated, and sites of phosphorylation have been identified (for review, see Hurley et al. 1998). We have developed a method for determining the degree and site specificity of rhodopsin phosphorylation in vivo using less than one-half of one mouse retina per analysis. This method can be used to quantitatively characterize the kinetics of rhodopsin phosphorylation within the mouse retina.

As shown in Figure 1, our method reliably detects 10 fmole of monophosphorylated rhodopsin peptide, which corresponds to 0.002% of the total rhodopsin in the mouse retina. The sensitivity of the instrument to the rhodopsin C-terminal peptide is linear over a 10,000-fold range of concentration, from 10 fmole to 100 pmole. This linearity allows for relative ease in quantitation of the differently

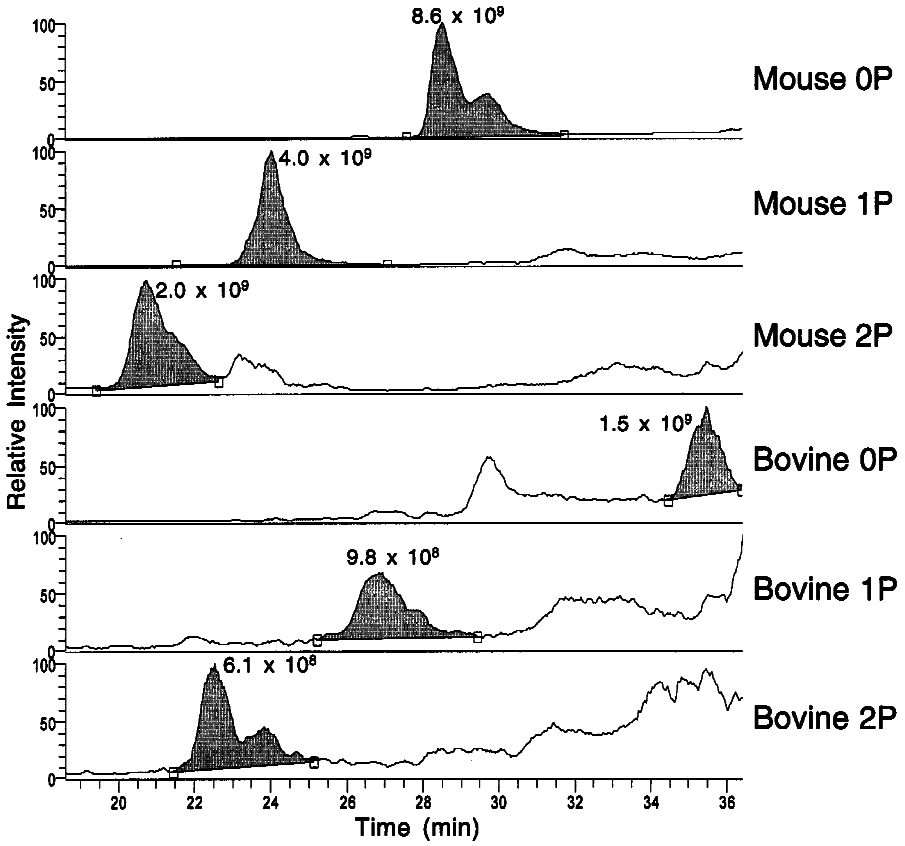

Fig. 6. LCMS of mouse rhodopsin peptides with bovine peptide internal standards. Ten microliters of light-exposed bovine ROS (~100 pmole rhodopsin) was added to a homogenate of the enucleated eye of a mouse that had been exposed to 1.0 mW/cm^2 illumination for 2 min according to our in vivo protocol. The x-axis represents elution time, and the y-axes are intensity of signal. The ion chromatograms pictured represent the same LCMS run, with the data divided into different mass windows. Each panel represents a different phosphorylated form, from zero (0P) to two (2P) phosphates, of either the mouse sample peptides or the bovine standard peptide. All monitored ions are doubly charged. The peak areas were integrated, with the area displayed above the peak.

phosphorylated species and indicates that the instrument is not being saturated at these concentration levels.

To account for the sensitivity of the mass spectrometer and accurately determine the relative amounts of the different phosphorylated species present in a retinal sample, we determined sensitivity coefficients for rhodopsin peptides phosphorylated on one to five sites. Furthermore, we developed LCMS/MS methodology for determining the sites of phosphorylation of singly and doubly phosphorylated rhodopsin peptides. We also developed a method to quantify the fractions of monophosphorylated species that are phosphorylated on each site.

Our data indicate that the most favored sites for rhodopsin phosphorylation are the three serine residues near the rhodopsin C terminus. The predominant phosphorylation site changes with time after the flash is administered, likely because of the site preferences of the kinase and phosphatase (Kennedy et al. 2001). The mouse rhodopsin C terminus also contains three threonines that are potential sites of phosphorylation. Indeed, we observe rhodopsin peptides with four and five phosphates (Fig. 8) at high bleach levels, which indicates phosphorylation of threonine residues. We are also able to observe low levels of monophosphorylation on threonine, notably Thr 340, which has been implicated in arrestin-mediated deactivation of rhodopsin (Zhang et al. 1997; Brannock et al. 1999). However, we do not have evidence for more than very low levels of threonine phosphorylation.

We have shown our method by analyzing mouse retinal rhodopsin samples generated by two types of protocols, the rapid-quench protocol and the in vivo protocol. Samples generated from both protocols showed an increase in total phosphorylation levels, as well as an increase in the relative amounts of each of the more highly phosphorylated species, with brighter light exposure. By both methods we observe low, but detectable, levels of rhodopsin monophosphorylation in samples that were not light exposed. This dark phosphorylation, rather than instrumental limitations, is the factor that limits our sensitivity of detection at low light levels. Neither protocol produced levels of rhodopsin phosphory-

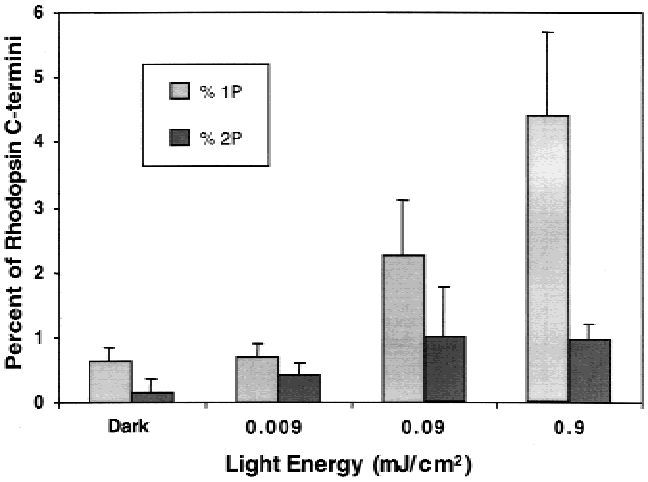

Fig. 7. Demonstration of rapid-quench method. Total signal was calculated by adding the integrated signals for unphosphorylated, singly, and doubly phosphorylated rhodopsin peptide, each corrected for differences in efficiency of detection. The plotted values are the percentage of this total rhodopsin peptide signal caused by singly (1P) and doubly (2P) phosphorylated rhodopsin at each indicated light intensity. These data have not been adjusted with bovine internal standards. Error bars represent standard deviation from three experiments.

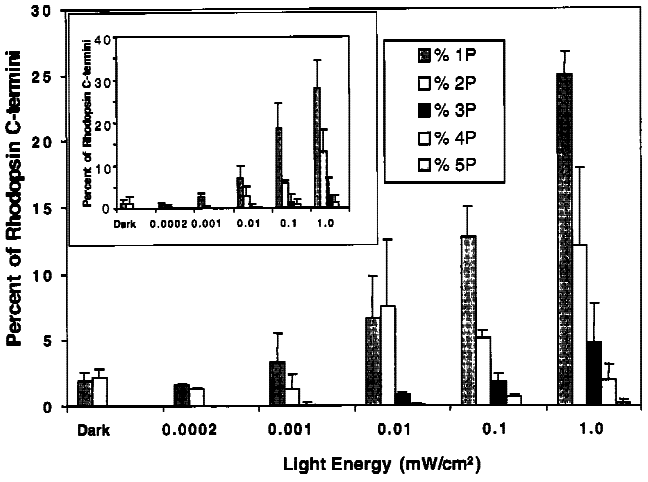

Fig. 8. Demonstration of in vivo method. Total signal was calculated by adding the integrated signals for unphosphorylated and each observed phosphorylation state of the rhodopsin peptide, each corrected for differences in efficiency of detection. The plotted values are the percentage of this total rhodopsin peptide signal caused by rhodopsin peptides with one (1P), two (2P), three (3P), four (4P), and five (5P) sites of phosphorylation at each indicated light intensity. (*inset*) The same data, after adjusting with internal standards. Light-exposed bovine ROS were added to each sample, and the mass spectrometric signal from each phosphorylated form of the bovine peptide was recorded. The bovine signal was used to normalize the mouse signal for each phosphorylated form of the peptide, and the adjusted data were replotted with error bars representing standard deviation of three experiments.

lation that were significantly greater than this dark phosphorylation level when using light levels less than 0.001 mW/cm^2.

Inclusion of light-exposed bovine ROS as an internal standard did not significantly improve the consistency of the results (Fig. 8, *inset*). This is not entirely unexpected. If our method relied on absolute quantitation of the amount of phosphorylated rhodopsin peptides in the mouse retina, use of internal standards would likely be essential. Because we are determining the percentage of phosphopeptide relative to the total amount of rhodopsin peptide, internal standards are only useful if they can correct for a differential effect on the phosphorylated versus the unphosphorylated peptide. Because the internal standard did not decrease the variability of the data, we conclude that no significant losses are occurring preferentially to one phosphorylated form over another through the course of the sample processing.

Before the development of our method, one report was published describing rhodopsin phosphorylation analysis in vivo (Ohguro et al. 1995). In that study, only monophosphorylated rhodopsin was detected, whereas by our method multiply phosphorylated rhodopsin was detected under all conditions of analysis. The method we have presented is more than two orders of magnitude more sensitive than the Ohguro method, because of the use of mass spectrometry as the detection method rather than absorbance. We typically use less than one retina per analysis, whereas more than 100 retinas were necessary for each of the earlier in vivo experiments. This greater sensitivity allows us to observe phosphorylated forms that were previously undetected. Recently, Ablonczy et al. (2000) also have reported multiple phosphorylation of rhodopsin under in vivo conditions.

We also improved the time resolution of the method to analyze the phosphorylation state of rhodopsin on a subsecond time scale. This allowed detection of phosphorylated species that may be degraded quickly by endogenous phosphatase activity. The quenching protocol we have developed uses 8 M urea and rapid homogenization that improve reaction quenching efficiency. It is possible that residual phosphatase activity dephosphorylated rhodopsin on Ser 343 in the previous study (Ohguro et al. 1995).

The methods described in this report have been used to elucidate the kinetics of rhodopsin phosphorylation in vivo and will be used in future studies aimed at the further characterization of the mechanisms of rhodopsin phosphorylation under conditions of both light and dark adaptation. These methods, with only slight modification, also could be applied to other known phosphoproteins. The method for partially purifying the C-terminal phosphopeptide, ultracentrifugation and Asp-N digestion to release the peptide from the membranes, could be useful for other phosphorylated GPCRs but would likely need to be modified for most phosphoproteins. If another protocol is used, one should take care that the protease cleaves the key sites with equal effi-

ciency regardless of phosphorylation state. If titration of the protease concentration yields peptides with consistent ratios of the various phosphorylation states, the protease must be cleaving them with equal efficiency. If not, analysis of percent phosphorylation will be complicated, and the use of a different protease may be appropriate.

For the kinetic studies using this methodology (Kennedy et al. 2001) and the light titration studies in Figures 7 and 8, we injected ~20 pmole rhodopsin peptide per sample. Because rhodopsin is highly abundant in the mouse retina, it was not difficult to obtain large amounts of peptide for analysis. However, we estimate that the same studies could be conducted with high femtomole quantities of total peptide if care is taken that the mass spectrometer is operating at peak condition. Monophosphorylated peptides were readily detectable at low femtomole quantities (Fig. 1) and were typically present at ~1% of the total rhodopsin peptide. Additionally, we have obtained useful data in these experiments from samples in which the total rhodopsin peptide signal was 1–2% of the signal we typically observe (data not shown). If more than one phosphorylation site per peptide is being monitored, the amount of phosphopeptide necessary for these types of studies will be greatly influenced by the efficiency of generation of useful collision-induced dissociation (CID) spectra from the phosphopeptide. The peptide used in this study is 19 amino acids and does not fragment as well as most standard peptides in the ion trap. If a smaller and more easily fragmented phosphopeptide were studied, one might expect useful data from mid- to low-femtomole levels of total peptide.

Materials and methods

Sample preparation for rapid-quench experiments

Samples were prepared using a protocol very similar to that described in Kennedy et al. (2001). For all samples, mice were dark-adapted overnight, and all steps through the addition of urea solution and homogenization were conducted under infrared illumination using night-vision goggles. For rapid-quench experiments, the samples were generated from dissected retinas. A mouse was sacrificed by cervical dislocation, both eyes were removed, and the retinas were dissected into oxygenated Locke's solution (140 mM NaCl, 0.6 mM KCl, 1.2 mM $CaCl_2$, 2.4 mM $MgCl_2$, 3 mM HEPES at pH 7.4, 10 mM glucose) at 37°C. The retinas and solution were transferred to the sample tube of the rapid-quench apparatus described in Kennedy et al. (2001). This apparatus was built in our laboratory and was designed to quickly terminate the rhodopsin phosphorylation reaction. A flash was administered from a Canon 540EZ Speedlite flash unit attenuated with filters of optical density 0.5–4.0 to provide a flash of the appropriate intensity. Two seconds after the flash, a solenoid valve was activated for 700 msec to allow 600–800 μL of 7 M deionized urea, 5 mM ethylenediamine-tetraacetic acid (EDTA), 20 mM Tris at pH 7.4 to flow into the sample tube. Simultaneously, a solenoid was activated to push the tube for 700 msec onto the tip of an UltraTurrax homogenizer rotating at 20,000 rpm. The sample then was frozen on dry ice.

The samples were thawed at 37° C, and membranes were pelleted by ultracentrifugation at 45 Krpm for 20 min using a Beckman TLA-55 rotor in a tabletop Beckman Optima ultracentrifuge. Membranes were washed twice with 10 mM HEPES at pH 7.4 and resuspended in 20 μL of 20 μg/mL Asp-N (Roche) in 10 mM HEPES at pH 7.4 and incubated for 17 h at room temperature while rocking. We determined the concentration of Asp-N to use in our experiments after performing a titration from 5 to 40 μg/mL Asp-N, optimizing for yield of rhodopsin C-terminal peptides. The percent phosphorylation detected was independent of Asp-N concentration over the upper range that was tested (20–40 μg/mL). The membranes again were pelleted by centrifugation for 20 min at 45 Krpm, and the peptides that had been released from the membrane were collected in the supernatant. The supernatant was diluted with water to 90 μL, and 10 μL 5% acetic acid was added to acidify the sample. The samples were stored at −20° C until they were analyzed. Before loading onto the HPLC, each sample was centrifuged in an Eppendorf 5415C microfuge for 10 min at 13,000 rpm. Approximately 10% yield of rhodopsin peptide was attained.

Sample preparation of in vivo experiments

For experiments conducted completely in vivo, dark-adapted mice were anesthetized with an intraperitoneal injection of ketamine and xylazine (140 mg/Kg and 0.5 mg/Kg body weight, respectively). One pupil was dilated by applying tropicamide and phenylephrine ~10 min before light exposure. The mouse was placed on a glass manifold connected to a 37° C circulating water bath. For 2 min, light from a halogen lamp, attenuated through filters of optical density 1–4, was focused on the cornea through a fiber optic cable and lens. The unattenuated intensity at the cornea was 1 mW/cm^2. After removing the light stimulus, the mouse was quickly sacrificed by cervical dislocation, and the light-exposed eye was removed and placed in the sample tube with 700 μL 7 M deionized urea, 5 mM EDTA, 20 mM Tris at pH 7.4. Thirty seconds after removal of the light stimulus, the eye was homogenized as described for the isolated retinas. Samples were processed as described above.

Standard peptides

Four different synthetic mouse rhodopsin C-terminal peptides were used in this study, including unphosphorylated and three monophosphorylated species, with phosphoserine at position 334, 338, or 343. All were prepared by Anaspec. The unphosphorylated and pS338 peptides were prepared with ^{13}C at the α-C of each alanine residue, so their mass is greater than the wild-type peptide and the pS334 and pS343 synthetic peptides by 5 a.m.u. The synthetic peptides were all quantified in duplicate by amino acid analysis (AAA Laboratory). Amino acids were analyzed by post-column derivatization with ninhydrin using a Beckman System 6300 updated to 7300-amino-acid analyzer (Beckman Instruments, Inc.). Between 4 and 40 nmole of each peptide was analyzed.

To determine the efficiency of mass spectrometric detection of multiply phosphorylated rhodopsin peptides, we purified C-terminal peptides of phosphorylated bovine rhodopsin. Bovine ROSs were purified and bleached under direct illumination of a TQ/FOI-1 halogen lamp (Techni-Quip Corp.) with a 21-V 150-W EKE bulb (General Electric Co.) for 1 h, with initial concentrations of 16 mM ATP and 1.3 mM GTP. Additional ATP and GTP were both added 20 and 40 min into the reactions, for final concentrations of 27 mM ATP and 2.2 mM GTP. Seven molar urea was added to stop the reactions, and rhodopsin C-terminal peptides

were isolated by Asp-N digestion and centrifugation, as described above for mouse samples. These peptides were separated by reversed-phase HPLC (buffer A: 0.06%TFA in water; buffer B: 0.052% TFA in 80% acetonitrile 20%water) into unphosphorylated and individual multiply phosphorylated fractions. One to 7 nmole of each species was quantified by amino acid analysis, with the peptides with four and five phosphates analyzed in duplicate (AAA Laboratory).

The purity of the bovine peptides was assessed by reversed-phase HPLC using a Vydac C18 commercial column, 20 cm length, no. 218TP54. The peptides were detected at 214 nm using the same mobile phase and gradient protocol that was used to purify the peptides. This HPLC protocol easily separated phosphopeptides that differed only in their sites of phosphorylation. To determine the purity of the peptides, we integrated the signal from the primary component of each peptide sample and divided it by the total signal from all peptide components that were detectable in the sample. By this method, the unphosphorylated peptide was found to be 91% pure, the monophosphorylated peptide was 87% pure, and the doubly phosphorylated peptide was 84% pure. We did not have enough pure bovine peptides with three and four phosphates to analyze them for purity by absorbance spectroscopy, and the purified bovine peptide with five phosphates was found to contain multiple species with different sites of phosphorylation that each eluted as distinct peaks. The presence of these multiple species prohibited our differentiating between contaminants and the peptides of interest.

The purity of the bovine peptides with three, four, and five phosphates was assessed by mass spectrometry. Each of the purified and quantified peptides was infused directly into the mass spectrometer, and the spectrum was recorded. The efficiencies of detection of the bovine peptides calculated using equation 1 were used to correct the amount of signal detected for each phosphopeptide mass to accurately reflect the amount of any contaminating rhodopsin phosphopeptides in the sample. We integrated the total signal for the primary component (including signal arising from salt adducts of the primary component) and divided that by the total integrated signal to determine the percent purity. By this method, we found the triply phosphorylated peptide to be 95% pure, the quadruply phosphorylated peptide to be 87.5% pure, and the quintuply phosphorylated peptide to be 100% pure. By both methods of purity analysis, some peptides contained other bovine rhodopsin phosphopeptides as contaminants. The amounts of these were noted and corrected for in the final analysis.

Using these data regarding the purity of the bovine phosphopeptide standards, we changed the concentration of each peptide species present in the standard peptide mixture analyzed in Figure 2, C and D. Adjusting the peptide concentrations affected the observed relative sensitivities, and these new, corrected values were plotted in Figure 2D.

Light-exposed bovine ROS for use as an internal standard was generated by the above protocol, but after the phosphorylation reaction was completed, the ROS were aliquoted and frozen at −70° C without further processing. Ten microliters of the ROS (8 μg rhodopsin) was added to each mouse sample before ultracentrifugation. Rhodopsin in ROS preparation was quantified by absorbance spectroscopy at 500 nm, using an extinction coefficient of 40,000 L $mole^{-1}$ cm^{-1} (Zimmerman and Godchaux 1982).

LCMS

Twenty-microliter samples were injected with a Perkin-Elmer ISS 100 autosampler onto a capillary column of 260 μm internal diameter (ID) and 5–15 cm in length with a total column volume of ~5 μL. These columns were packed at 500–800 p.s.i. using Vydac C182TP reversed-phase resin in 50% methanol. The columns immediately were acidified with 0.5% acetic acid. Samples were loaded onto the column at a flow rate of 3–5 μL/min, and peptides were eluted at 2–4 μL/min with column pressure of ~350 p.s.i. at ambient temperature. The peptides were loaded in 0.08% heptafluorobutyric acid (HFBA) and typically eluted in 0.08% HFBA 10% acetonitrile. The acetonitrile concentration required for phosphopeptide elution was variable, depending on column length, column pressure, flow rate, and possibly other variables, such as temperature. All rhodopsin phosphopeptides in each sample were eluted isocratically in ~10% acetonitrile, and the acetonitrile concentration was increased by 5%–10% to elute the unphosphorylated rhodopsin C-terminal peptide. The acetonitrile concentration then was stepped up to 80% for 10 min to elute the remaining sample peptides that were not relevant to our studies. The HPLC method was optimized daily by observing peptide elution patterns and making appropriate adjustments. The total HPLC run time, including column equilibration, was 65 minutes.

Sample was delivered to the mass spectrometer using a microspray apparatus built in the laboratory (Figeys et al. 1998) with commercial needles of either 8 or 15 μm ID (New Objective, Inc.). For all experiments, we used the ThermoFinnigan LCQ Deca ion trap mass spectrometer in positive ion mode. The instrument was tuned at least monthly using the pS338 synthetic peptide. Tuning was performed more often if sensitivity decreased or if cleaning of the instrument was necessary. CID analyses of monophosphorylated peptides were performed using activation amplitude of 20.5%, activation Q of 0.250, activation time of 50 msec, and isolation width of 2.5 m/z. CID of doubly phosphorylated species was performed with activation amplitude of 28%, whereas all other parameters were the same as those used for monophosphorylated peptides.

pH experiment

The pH of the three solutions analyzed was determined using an Orion model 720A pH meter calibrated using commercial calibrating solution at pH 4.00 and standard solution at pH 2.00 (25 mL 0.2 M KCl + 6.5 mL 0.2 M HCl; Lide 1992). All three solutions contain 10 pmole/μL bovine unphosphorylated rhodopsin C-terminal peptide, 10 pmole/μL bovine C-terminal peptide with five phosphates, and 10% acetonitrile. Solution at pH 2.2 contained 0.24% HFBA, solution at pH 2.6 contained 0.06% HFBA, and solution at pH 3.3 contained water only. The solutions were analyzed by directly infusing them into the mass spectrometer at 1 μL/min using standard mass spectrometric settings.

Acknowledgments

These studies were performed using funds from the Howard Hughes Medical Institute and NIH grant EY06641 (JBH).

The publication costs of this article were defrayed in part by payment of page charges. This article must therefore be hereby marked "advertisement" in accordance with 18 USC section 1734 solely to indicate this fact.

References

Ablonczy, Z., Knapp, D.R., Darrow, R., Organisciak, D.T., and Crouch, R.K. 2000. Mass spectrometric analysis of rhodopsin from light damaged rats. *Mol. Vis.* **6:** 109–115.

Adams, M.D., Celniker, S.E., Holt, R.A., Evans, C.A., Gocayne, J.D., Amanatides, P.G., Scherer, S.E., Li, P.W., Hoskins, R.A., Galle, R.F. et al. 2000. The genome sequence of *Drosophila melanogaster*. *Science* **287:** 2185–2195.

Annan, R.S. and Carr, S.A. 1996. Phosphopeptide analysis by matrix-assisted laser desorption time-of- flight mass spectrometry. *Anal. Chem.* **68:** 3413–3421.

Brannock, M.T., Weng, K., and Robinson, P.R. 1999. Rhodopsin's carboxyl-terminal threonines are required for wild-type arrestin-mediated quench of transducin activation in vitro. *Biochemistry* **38:** 3770–3777.

Carr, S.A., Huddleston, M.J., and Annan, R.S. 1996. Selective detection and sequencing of phosphopeptides at the femtomole level by mass spectrometry. *Anal. Biochem.* **239:** 180–192.

Figeys, D., Gygi, S.P., Zhang, Y., Watts, J., Gu, M., and Aebersold, R. 1998. Electrophoresis combined with novel mass spectrometry techniques: Powerful tools for the analysis of proteins and proteomes. *Electrophoresis* **19:** 1811–1818.

Goshe, M.B., Conrads, T.P., Panisko, E.A., Angell, N.H., Veenstra, T.D., and Smith, R.D. 2001. Phosphoprotein isotope-coded affinity tag approach for isolating and quantitating phosphopeptides in proteome-wide analyses. *Anal. Chem.* **73:** 2578–2586.

Graves, J.D. and Krebs, E.G. 1999. Protein phosphorylation and signal transduction. *Pharmacol. Ther.* **82:** 111–121.

Hunter, T. and Plowman, G.D. 1997. The protein kinases of budding yeast: Six score and more. *Trends Biochem. Sci.* **22:** 18–22.

Hurley, J.B., Spencer, M., and Niemi, G.A. 1998. Rhodopsin phosphorylation and its role in photoreceptor function. *Vision Res.* **38:** 1341–1352.

Kennedy, M.J., Lee, K.A., Niemi, G.A., Craven, K.B., Garwin, G.G., Saari, J.C., and Hurley, J.B. 2001. Multiple phosphorylation of rhodopsin and the in vivo chemistry underlying rod photoreceptor dark adaptation. *Neuron* **31:** 87–101.

Koch, C.A., Anderson, D., Moran, M.F., Ellis, C., and Pawson, T. 1991. SH2 and SH3 domains: Elements that control interactions of cytoplasmic signaling proteins. *Science* **252:** 668–674.

Lide, D.R. 1992. CRC handbook of chemistry and physics, 73d ed. CRC Press, Inc., Boca Raton, FL.

Neubauer, G. and Mann, M. 1999. Mapping of phosphorylation sites of gel-isolated proteins by nanoelectrospray tandem mass spectrometry: Potentials and limitations. *Anal. Chem.* **71:** 235–242.

Oda, Y., Huang, K., Cross, F.R., Cowburn, D., and Chait, B.T. 1999. Accurate quantitation of protein expression and site-specific phosphorylation. *Proc. Natl. Acad. Sci.* **96:** 6591–6596.

Oda, Y., Nagasu, T., and Chait, B.T. 2001. Enrichment analysis of phosphorylated proteins as a tool for probing the phosphoproteome. *Nat. Biotechnol.* **19:** 379–382.

Ohguro, H., Van Hooser, J.P., Milam, A.H., and Palczewski, K. 1995. Rhodopsin phosphorylation and dephosphorylation in vivo. *J. Biol. Chem.* **270:** 14259–14262.

Palczewski, K., Buczylko, J., Kaplan, M.W., Polans, A.S., and Crabb, J.W. 1991. Mechanism of rhodopsin kinase activation. *J. Biol. Chem.* **266:** 12949–12955.

Plowman, G.D., Sudarsanam, S., Bingham, J., Whyte, D., and Hunter, T. 1999. The protein kinases of *Caenorhabditis elegans*: A model for signal transduction in multicellular organisms. *Proc. Natl. Acad. Sci.* **96:** 13603–13610.

Resing, K.A. and Ahn, N.G. 1997. Protein phosphorylation analysis by electrospray ionization-mass spectrometry. *Methods Enzymol.* **283:** 29–44.

Vener, A.V., Harms, A., Sussman, M.R., and Vierstra, R.D. 2001. Mass spectrometric resolution of reversible protein phosphorylation in photosynthetic membranes of *Arabidopsis thaliana*. *J. Biol. Chem.* **276:** 6959–6966.

Wilm, M., Neubauer, G., and Mann, M. 1996. Parent ion scans of unseparated peptide mixtures. *Anal. Chem. 68:* 527–533.

Zhang, L., Sports, C.D., Osawa, S., and Weiss, E.R. 1997. Rhodopsin phosphorylation sites and their role in arrestin binding. *J. Biol. Chem.* **272:** 14762–14768.

Zhou, H., Watts, J.D., and Aebersold, R. 2001. A systematic approach to the analysis of protein phosphorylation. *Nat. Biotechnol.* **19:** 375–378.

Zimmerman, W.F. and Godchaux, W. 1982. Preparation and characterization of sealed bovine rod cell outer segments. *Methods Enzymol.* **81:** 52–57.